Kelvin probe spectroscopy of a two-dimensional electron gas below 300 mK

T. Vančura, S. Kičin, T. Ihn, and K. Ensslin[a]
Solid State Physics Laboratory, ETH Zurich, 8093 Zurich, Switzerland

M. Bichler
Walter Schottky Institute, 85748 Garching, Germany

W. Wegscheider
Institute for Applied and Experimental Physics, University of Regensburg, 93040 Regensburg, Germany

A scanning force microscope with a base temperature below 300 mK is used for measuring the local electron density of a two-dimensional electron gas embedded in a Ga[Al]As heterostructure. At different separations between atomic force microscope tip and sample, a dc voltage is applied between the tip and the electron gas while simultaneously recording the frequency shift of the oscillating tip. Using a plate capacitor model, the local electron density can be extracted from the data. The result coincides within 10% with the data obtained from transport measurements. © *2003 American Institute of Physics.* [DOI: 10.1063/1.1614836]

The electron density of two-dimensional electron gases (2DEGs) is usually determined by magnetotransport experiments. The carrier density can be either extracted from the low-field slope of the Hall resistance or from the $1/B$ periodicity of Shubnikov-de Haas oscillations. In addition, $C-V$ profilometry[1-4] and magnetocapacitance experiments[5,6] are versatile tools to detect the electron density in an electron gas located below a metallic top-gate electrode.

Here, we set out to use a Kelvin probe technique in order to measure the local electron density in a 2DEG below the conductive tip of an atomic force microscope.

The 2DEG investigated is embedded in a Ga[Al]As heterostructure with the electrons buried 40 nm below the surface. No mesa structure was imprinted. Ohmic contacts at the sample edges allow us to measure the four-terminal resistances at low temperatures and to determine the carrier density through transport measurements.

The sample is mounted in a home-built scanning probe microscope (SPM) situated in a ^{3}He-cryostat[7] in which an operating temperature below 300 mK is reached routinely. Scanning is performed with an electrochemically etched metallic tip attached to the end face of one prong of a piezoelectric quartz tuning fork.[8-12]

Optical detection of the cantilever deflection is not suitable for our purposes, because the sample's electronic properties are sensitive to light (persistent photoeffect). Therefore the setup relies on a piezoelectric measurement of the tip oscillation utilizing a phase-locked loop measuring the change in resonance frequency upon changes in the tip–sample interaction.[13,14] The relative accuracy of the frequency detection is better than 10^{-7}.[7,11,15]

In a dynamic mode SPM at small tip-oscillation amplitudes, the measured frequency shift Δf does not directly reflect the force F_{ts} acting on the cantilever, but rather the force gradient[13]

$$\Delta f \propto \frac{dF_{ts}}{dz} =: F'_{ts}. \tag{1}$$

By applying a dc voltage between the metallic tip and the sample, the density is modified. In a metallic system one expects a parabolic voltage dependence of the force gradient. The curvature of the parabola is determined by the capacitive coupling between tip and sample. The position of the apex of the parabola determines the contact potential difference U_{CPD} of the two metals. This method is generally known as Kelvin probe.[16-18]

Figure 1 shows Kelvin probe data measured at different tip–sample distances with a 2DEG below the tip. The curvature of the measured curves is different for positive and negative voltages as indicated by the fit to the 9-nm curve. The reason lies in the depletion of the electron gas below the tip for positive voltages. This changes the tip–sample capacitance and thus reduces the force coupling.
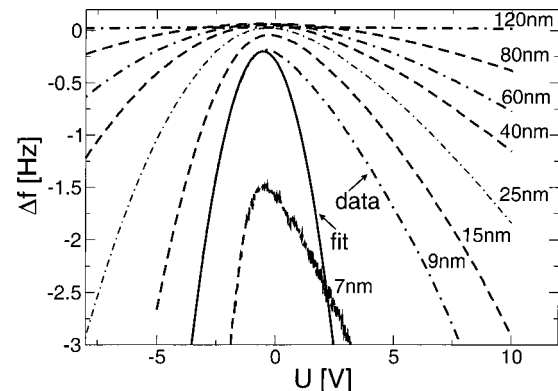

FIG. 1. Kelvin probe at different tip–sample distances. On the vertical axis the frequency shift Δf is plotted versus the bias voltage U on the horizontal axis. The solid line indicates the parabolic fit to the data taken at 9-nm tip–sample separation. We choose the sign of the voltage always with respect to the 2DEG; that is, a negative voltage indicates that the negative contact is connected to the electron gas.
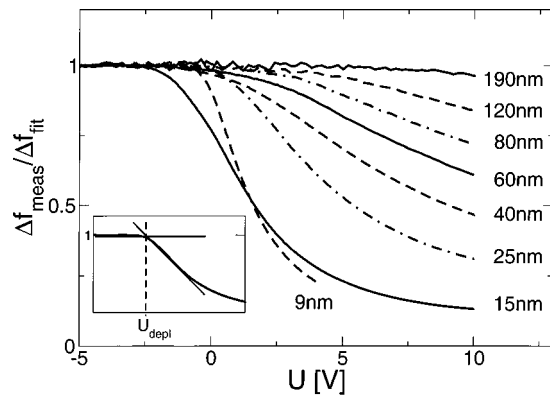
[a]Electronic mail: ensslin@phys.ethz.ch

FIG. 2. Relative Kelvin probe. The data from Fig. 1 are divided by their respective parabolic fit. Inset: The position where the depletion sets in (U_{depl}) is defined as indicated in the inset, as the point where the tangent to the curve crosses the $y=1$ axis.

The electrostatic force gradient F'_{ts} between tip and sample responds to a change in the bias voltage U as

$$F'_{ts} = \frac{1}{2} \frac{d^2 C(z,U)}{dz^2}(U - U_{CPD})^2, \qquad (2)$$

where $C(z,U)$ is the tip–sample capacitance. For metallic samples, $C(z,U)$ is independent of U and the maximum of the parabola is shifted in voltage by U_{CPD}. The experiments were performed after a series of image scans. The tip was not very sharp, increasing the tip–sample capacitance.

The solid line in Fig. 1 shows a parabolic fit to the 9-nm trace. At negative bias voltages, the fit was made to agree well with the data; that is, in the regime in which the electron gas is not depleted. At positive voltages, however, at which the electron gas becomes depleted and the tip–sample coupling is weakened due to the voltage dependence of $d^2 C(z,U)/dz^2$, the curvature is reduced. Already in Fig. 1, a relation between the point, where the depletion sets in, and the tip–sample distance can be seen. This point of depletion will be the focus of the following discussion.

In order to determine U_{depl} quantitatively, the ratio $\Delta f_{meas}/\Delta f_{fit}$ is evaluated as a function of U (see Fig. 2). We define the depletion voltage U_{depl} as the position of the knee in $\Delta f_{meas}/\Delta f_{fit}$ determined as shown in the inset of Fig. 2. These depletion voltages are plotted versus the respective tip–sample separation in Fig. 3(a). The broken line is a linear fit to the data.

We approximate our setup with a plate capacitor model to extract a local electron sheet density n_s from this data. One capacitor plate, the tip, resides at a distance z above the sample surface. The 2DEG is buried underneath a GaAs cap layer of thickness D. The dielectric constants are $\epsilon_1 = 1$ for the vacuum and $\epsilon_2 = 12$ for GaAs [see inset in Fig. 3(a)].

For $U < U_{depl}$, the total capacitance $C_{tot}(z)$ is assumed to be independent of voltage and given by

$$\frac{C_{tot}(z)}{A} = \frac{\epsilon_0 \epsilon_1 \epsilon_2}{\epsilon_2 z + \epsilon_1 D},$$

where A is the area of the plates.

The charge density in the 2DEG is given by

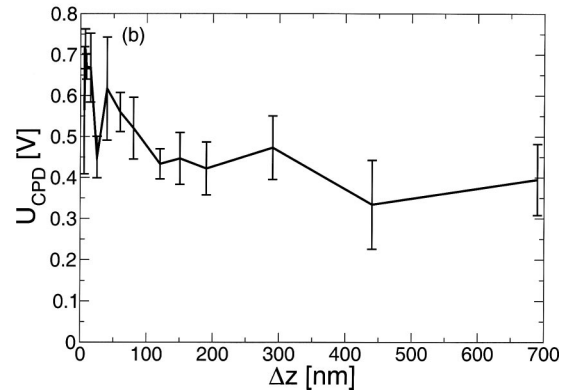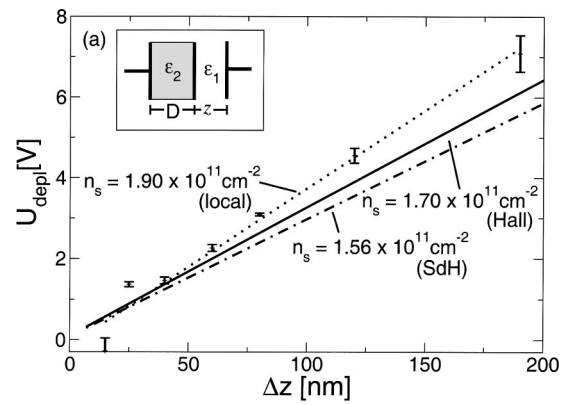$$en_s(U) = \frac{\Delta Q}{A} = -\frac{C_{tot}}{A}(U - U_{CPD}) + en_s^{(0)},$$

FIG. 3. (a) Depletion voltage plotted versus the tip–sample distance at which the Kelvin probe was recorded. The electron density extracted from the transport data is $n_{Hall} = 1.70 \times 10^{11}$ cm^{-2} and $n_{SdH} = 1.56 \times 10^{11}$ cm^{-2}. This leads to the solid lines in the graph. Inset: Model geometry. (b) Contact potential difference U_{CPD} plotted as a function of Δz.

where $n_s^{(0)}$ is the charge carrier density for $U = U_{CPD}$ and $n_s(U)$ is the voltage dependent charge carrier density in the 2DEG underneath the tip.

For total depletion under the tip, $n_s(U_{depl}) = 0$ and the depletion voltage is

$$U_{depl} = U_{CPD} + \frac{e n_s^{(0)}}{\epsilon_0 \epsilon_1 \epsilon_2}(\epsilon_1 D + \epsilon_2 z); \qquad (3)$$

that is, there is a linear dependence between depletion voltage and tip–sample separation Δz. The free parameter determining the slope of $U_{depl}(z)$ is the electron density $n_s^{(0)}$ of the 2DEG.

From the data plotted in Fig. 3(a), a local electron density of $n_s^{local} = 1.9 \times 10^{15}$ m^{-2} is extracted from the slope of the data points. This compares to the electron densities obtained from Shubnikov–de Haas and Hall transport measurements. They are $n_{Hall} = 1.70 \times 10^{-15}$ m^{-2} and $n_{SdH} = 1.56 \times 10^{-15}$ m^{-2}. The corresponding curves in Fig. 3(a) have been generated using Eq. (3).

The three results differ slightly. Considering that the methods and scopes of the three measurements are different, this is not unexpected. The local measurement probes the local properties of the electron gas right underneath the tip whereas transport measurements average over the whole sample area. Scanning electron microscope images of the tip performed after warming suggest a tip radius R in the range of 1 μm. This is more than an order of magnitude larger than

the average tip–sample separation, and hence the plate capacitor model is justified.

When talking about local measurements, the question of the lateral resolution arises. We have not yet performed scanning capacitance experiments with the described method, but as the method relies on $R \gg \Delta z$, the resolution will be limited by the tip radius R.

The contact potential difference U_{CPD} between the PtIr tip and the 2DEG can be extracted from positions of the maxima of the fitted parabolas. In Fig. 3, we plot U_{CPD} versus the tip–sample separation. There is a slight decrease of U_{CPD} with Δz. The typical value for U_{CPD} for a PtIr-heterostructure system is 0.5 V as measured. This value is important because it has to be taken into account in noninvasive electronic measurements.

The high stiffness of our tuning fork oscillator is the basis for the presented measurements. Although softer cantilevers suggest a higher force resolution, they bend with attracting forces and Δz would no longer be constant. At higher forces, the tip on a soft cantilever would even stick to the sample in what is generally known as "snap-in."

A general model not reproduced here involving doping ions and surface charges adds a distance dependence to the expression for U_{CPD}. Reducing it to a plate capacitor cancels out this dependence.

In conclusion, we have performed low-temperature local Kelvin probe measurements on a Al[Ga]As heterostructure using a tuning-fork-based scanning probe microscope. With the help of a plate capacitor model, the local electron density underneath the tip could be determined.

[1] T. Ambridge, C. R. Elliott, and M. M. Faktor, J. Appl. Electrochem. **3**, 1 (1973).

[2] P. Blood, Semicond. Sci. Technol. **1**, 7 (1986).

[3] P. J. Baxandall, D. J. Colliver, and A. F. Fray, J. Phys. E **4**, 213 (1971).

[4] J. A. Copeland, IEEE Trans. Electron Devices **15**, 761 (1969).

[5] V. Mosser, D. Weiss, K. von Klitzing, K. Ploog, and G. Weimann, Solid State Commun. **58**, 1 (1986).

[6] T. H. Smith, B. B. Goldberg, M. Heiblum, and P. J. Stiles, Surf. Sci. **170**, 304 (1986).

[7] T. Ihn, *Electronic Quantum Transport in Mesoscopic Semiconductor Structures, Springer Tracts in Modern Physics* (Springer, Berlin, 2003) Vol. 192.

[8] P. Güthner, U. Ch. Fischer, and K. Dransfeld, Appl. Phys. B: Lasers Opt. **48**, 89 (1989).

[9] K. Karrai and R. D. Grober, Appl. Phys. Lett. **66**, 1842 (1995).

[10] H. Edwards, L. Taylor, W. Duncan, and A. J. Melmed, J. Appl. Phys. **82**, 980 (1997).

[11] J. Rychen, T. Ihn, P. Studerus, A. Herrmann, K. Ensslin, H. J. Hug, P. J. A. van Schendel, and H. J. Güntherodt, Appl. Surf. Sci. **157**, 290 (2000).

[12] F. J. Giessibl, Appl. Phys. B: Lasers Opt. **76**, 1470 (2000).

[13] T. R. Albrecht, P. Grütter, D. Horne, and D. Rugar, J. Appl. Phys. **69**, 668 (1991).

[14] U. Dürig, O. Züger, and A. Stalder, J. Appl. Phys. **72**, 1778 (1992).

[15] J. Rychen, T. Ihn, P. Studerus, A. Herrmann, K. Ensslin, H. J. Hug, P. J. A. van Schendel, and H. J. Güntherodt, Rev. Sci. Instrum. **71**, 1695 (2000).

[16] M. Nonnenmacher, M. P. o'Boyle, and H. K. Wickramasinghe, Appl. Phys. Lett. **58**, 2921 (1991).

[17] H. O. Jacobs, H. F. Knapp, and A. Stemmer, Rev. Sci. Instrum. **70**, 1756 (1999).

[18] W. Nabhan, B. Equer, A. Broniatowski, and G. De Rosny, Rev. Sci. Instrum. **68**, 3108 (1997).